ASME Open Journal of Engineering
Online journal at:
https://asmedigitalcollection.asme.org/openengineering

Effect of Filament Color and Fused Deposition Modeling/ Fused Filament Fabrication Process on the Development of Bistability in Switchable Bistable Squares

Katie A. Martin[1]
US Army Corps of Engineers Engineer Research and Development Center,
Vicksburg, MS 39180-9732
e-mail: katie.a.martin@usace.army.mil

Travis L. Thornell
US Army Corps of Engineers Engineer Research and Development Center,
Vicksburg, MS 39180-9732
e-mail: travis.l.thornell@usace.army.mil

Hayden A. Hanna
US Army Corps of Engineers Engineer Research and Development Center,
Vicksburg, MS 39180-9732
e-mail: hayden.a.hanna@usace.army.mil

Charles A. Weiss, Jr.
US Army Corps of Engineers Engineer Research and Development Center,
Vicksburg, MS 39180-9732
e-mail: charles.a.weiss@usace.army.mil

Zackery B. McClelland
US Army Corps of Engineers Engineer Research and Development Center,
Vicksburg, MS 39180-9732
e-mail: zackery.b.mcclelland@usace.army.mil

Switchable multistable structures (SMS) are additively manufactured metamaterials. SMS are printed in polylactic acid, a shape memory polymer, and pre-strain is stored in bilayers during fused deposition modeling 3D printing process that encode different stable states can be activated above the glass transition temperature (T_g). Eight filament colors were used to 3D print sample squares. A hot water bath was used to determine sample bistability or monostability. Differential scanning calorimetry determined the T_g and melting temperature, (T_m). Thermogravimetric analysis was used to investigate colored filament thermal stability. The viscoelasticity of colored filament was investigated with melt rheology and the crystallinity of the printed samples was studied with X-ray diffraction. Filament color was an indicator of bistability and colors with lower T_m values tended to be bistable. Polyethylene terephthalate glycol SMS exhibited the shape memory effect but did not show bistability with the given print parameters. Bistability is achieved when the difference between the pre-strain of the bilayers is less than the energy needed to snap the sample to a given state. The relationship between monostability, self-snapping back to a favored state, and bistability is explained by a series of mathematical equations. Future work includes printing pre-strain relationship and the molecular level impact. [DOI: 10.1115/1.4064142]

Keywords: color, 4D printing, 3D printing, additive manufacturing, metamaterials, bistability, switchable multistable structures (SMS), fused deposition modeling (FDM), fused filament fabrication (FFF), material characteristics, print paramaters, additives, applied mathematics, material characterization of polymers, materials and processes, materials testing, polymers

1 Introduction

ISO 17296-3:2014(E) defines additive manufacturing or 3D printing [1] as "a process of joining bulk raw materials to make parts from 3D model data, usually layer upon layer, as opposed to subtractive manufacturing and formative methodologies" [2]. 3D printing formats include material extrusion, binder jetting, and direct energy deposition [1,3]. Fused deposition modeling (FDM) is a type of material extrusion [1,3], and it is one of the most commonly used 3D printing techniques [1,4]. FDM printing creates a 3D object by heating thermoplastic filament above its melting temperature (T_m) and extruding it through a nozzle onto the print bed, where the object is built up one layer at a time [1,4–7]. FDM is also known as fused filament fabrication (FFF) [5]. Polylactic acid (PLA) is a common filament choice for FDM printing [5,7].

Four-dimensional (4D) printing is a subcategory of 3D printing. A 4D print is a 3D printed object that responds in a predictable, predetermined way to an external stimulus, with time as the fourth dimension [1,3,8]. A print may respond to an external stimulus such as temperature, water, and pH [1,3,8] by twisting, bending, or folding [8]. 4D printing has numerous applications: origami folding for storage [8], soft robotic components [1], and preprogrammed folding antennas [3].

A shape memory polymer (SMP) [6] is a material capable of responding to an outside stimulus, such as temperature, by changing shape. When an SMP is heated above its transition temperature (T_{trans}), it can be deformed from its programmed permanent shape into a temporary shape and then cooled. When the SMP is reheated above T_{trans}, the original permanent shape returns [9]. The shape memory effect (SME) [10] is a process reliant on material structure,

[1]Corresponding author.

Manuscript received November 2, 2023; final manuscript received November 17, 2023; published online January 4, 2024. Tech. Editor: Hameed Metghalchi.

chemical composition, and material processing [9,11]. SMPs have been used in 4D printing [1,6,7,12–15].

The polymer can return to the programmed shape because stretched polymers relax into a randomly coiled state [11]. (Lendlein and Kelch explain the SME for an elastomer [9]; however, given that Yahia et al. discuss a similar process in PLA [7,11,13], a shape memory polymer [7], some of the explanation supplied for thermoplastic elastomers also is assumed to cover PLA. This work will also focus on the physical net-points instead of chemical cross-linking [9,11].)

SMPs have two elements: shape-fixing and shape-switching [11,13]. The shape-fixing elements are physical net points formed by entanglements and crystallization from noncovalent bonds (such as hydrogen bonding or van der Waals forces) [11] and stabilize the permanent programed shape [9,11]. Located between the shape-fixing elements are long polymer chains that serve as the shape-switching elements [11,13]. These chains store elastic energy when stretched and release it during shape recovery [11,13]. In an amorphous material, at the same internal energy, the highest entropy configuration is a strongly coiled conformation. Entanglements can prevent chains from slipping past each other [9].

PLA is a thermoplastic [11] SMP [7]. High molecular weight PLA can exhibit the SME because crystallization and physical entanglement serve as shape-fixing elements [11]. The melting temperature (T_m) and glass transition (T_g) of PLA can be T_{trans}. PLA is glassy below T_g and deformable above T_g [13].

The process outlined below refers to 3D printed SMPs that have T_{trans} at T_g. Above T_g, polymer chains are free to rotate, [6,9,13] and enter new energetically equivalent configurations, often random coils [9]. Pre-strain is stored during the printing process as the polymer is stretched across the print bed [12] or previous layers into an energetically unfavorable state with low entropy in the direction of the nozzle [6,9]. Entanglements prevent immediate relaxation of the polymer chains [9]. If held above T_g, a new energy minimum is established [6,9]. If cooled quickly below T_g, as occurs during the 3D printing process, the polymer is frozen in an unfavorable state and a temporary shape results. When heated to an activation temperature (T_{act}) above T_g, the amorphous chains recoil and the permanent shape is achieved [6,11].

Print parameters that affect pre-strain storage include nozzle and print bed temperature, layer height, T_{act}, and print speed [6,7,12,14,15]. Higher temperatures nozzle temperatures allowed more time for amorphous chain relaxation and less pre-strain to be stored [7]. The FDM printing process creates a pre-strain gradient between the top layer, printed last, and the bottom layer, printed first directly on the print bed, where the bottom layer has the least pre-strain and the top layer has the most pre-strain. As new material is deposited, the material below is partially reheated and some pre-strain is lost [12,14,15]. Printing on a different surface from the rest of the layers may reduce the first layer pre-strain because the material may stretch differently [14]. The further a layer is from the heated bed, the less pre-strain will be lost [15]. Bodaghi et al.'s samples bent upward toward the top layer, indicating that pre-strain was the highest in the top layer [12].

3D printed polyethylene terephthalate glycol (PETG) can exhibit the SME [16,17]. Aberoumand et al. 3D printed samples and then used a customized universal tensile device to demonstrate the SME [17]. Soleyman et al. printed PETG samples that achieved desired shape change and reported that the pre-strain was higher in the lower layers for PETG [16].

The colorant chosen to color a plastic affects the resulting characteristics. Dyes can have a plasticizing effect, changing processing behavior. Some pigments affect the shrinkage behavior of a crystalline thermoplastic. Warpage, the uneven shrinking of a part, can be affected by organic pigments [18]. Furthermore, filament color affects the properties of 3D printed structures. Wittbrodt and Pearce showed that the filament color of PLA and the nozzle temperature of white PLA affected the crystallinity of the FDM printed part [19]. The color of the PLA affected the thermal properties [4,5], rheological properties, and crystallization of FDM printed parts [5].

Fig. 1 Eight filament sections corresponding to tested filament colors

Bistable mechanical systems have two stable states and a potential energy threshold that must be overcome to achieve snap-through [20]. Riley et al. developed switchable multistable structures (SMS) that could be switched between two or more stable states when heated above T_g and remained in the selected state or an arbitrary state when the temperature was below T_g [6]. The SMS were created by FDM printing PLA in specific controlled bilayers, including a switchable bistable square (60 mm × 60 mm × 1 mm) with two stable states. Pre-strain was stored during the extrusion process. Each bilayer had an equal number of printed layers, with the bilayers printed orthogonally to each other. The square was activated in a water bath above T_g [6]. See Fig. 1 from Riley et al. for a visual representation of SMS creation and usage [6].

This paper considers the switchable bistable squares presented by in Riley et al. [6]. Samples were printed and tested for bistability; then material characterization tests were run. Finally, a series of mathematical explanation is presented with a general explanation.

2 Materials and Methods

2.1 Filament and 3D Printing of Bistable Squares. Eight different filament colors (PLA, 1.75 mm) were studied: blue, black, clear pro, green, lime green, yellow, purple, and red. The clear filament was a pro series filament, while all other filaments were regular filament. The filament manufacturer did not disclose its colorant, colorant amount, or any additional additives. The clear pro filament could have additional additives not present in the other regular colors. The pro PLA has a tolerance of ±0.02 mm [21] and the regular PLA has a tolerance of ±0.05 mm [22]. Sections of each colored filament are shown in Fig. 1.

An FDM 3D printer with a brass 0.4 mm nozzle was used to print the samples. Parts were printed on a removable magnetic steel sheet [23]. Hairspray was used as an adhesive.

The switchable bistable square samples followed the switchable bistable square design created by Riley et al. [6]. A 60 mm × 60 mm × 1 mm square was created with a layer height of 0.01 mm for all layers. The first five layers were printed in the 0 deg direction and the last five layers were printed in the 90 deg direction. The nozzle temperature was 200 °C, and the print bed temperature was 60 °C. Three samples of each color were printed on the right side of the build plate.

The initial printed samples printed are not bistable. Riley et al. used blue PLA; the authors used black PLA from a different manufacturer. Riley et al. used a different FDM printer with a glass bed instead of a metal print bed. Riley et al. printed at 30 mm/s; the authors printed at 60 mm/s. The initial layer height and the line thickness were changed, the time between printing and testing was decreased, the print bed was cleaned between prints, and the

bed temperature was decreased to room temperature. Some changes were marginally successful, but none consistently created bistability. Blue PLA samples made following the original slicing parameters with the same differences listed above were bistable.

Samples were printed in sets of three across the middle of the bed with varying print parameters, including color, nozzle temperature, and print speed. Because location on the print bed affected the bistability exhibited in the samples, all color samples were reprinted on the same spot on the right side of the print bed, as were blue samples at nozzle temperatures 185 °C, 200 °C, and 210 °C. Samples that were printed with visible bumps or defects were discarded. The print bed was cleaned periodically; therefore, the hairspray thickness varied between prints and may have affected pre-strain storage in the first layer.

Two different stable states were encoded in the square samples. State 1 was encoded by printing a bilayer (bilayer0) in the 0 deg direction. State 1 was activated when bilayer0 was concave. Bilayer0 was printed on the bottom, closest to the print bed. State 2 was encoded by printing a bilayer (bilayer90) in the 90 deg direction. State 2 was activated when bilayer90 was concave. The samples were printed flat and were activated by raising the sample temperature above T_g. States were activated by snapping samples with tweezers.

Blue PETG samples from 1.75 mm diameter filament were also printed. Printer settings for the same as the PLA samples except for nozzle temperature set at 245 °C and print bed temperature at 85 °C. Samples were printed on the left, right, and middle of the print bed.

The filament manufacturer did not provide a T_g value for PLA or PETG [24,25]. A T_g of 60 °C was assumed for PLA [6,13]. A T_g of 80 °C was assumed for PETG [26].

2.2 Water Bath Heating Test. A water bath provided a consistent temperature to the entire sample. A T_{act} of 65 ± 1 °C was chosen because it is 5 °C above the glass transition temperature of PLA. A few seconds after heating, the sample would shift and snap to one of the possible states. If the sample got "stuck" between two states, tweezers were used to switch the sample to one of the states. Once the sample was fully snapped, it was snapped in the opposite direction. If the sample returned to the first state without intervention, the sample was considered monostable. Each sample was snapped back and forth between states, allowing 15 s or more between each state. If the sample stayed in the just-snapped orientation after three times, the sample was considered bistable. Some samples lost bistability when heat was applied too long and became stuck in the selected state, a phenomenon noted by Riley et al. [6], due to a new energy minimum being established [6,9]. The process of bistable square activation is shown in Fig. 2.

2.3 Differential Scanning Calorimetry. Differential scanning calorimetry was used to determine the T_g and the T_m of each filament color. Filament was dried overnight at 65 °C to remove any moisture. Small samples were cut from the dried section of filament, weighed, and then hermetically sealed. A heat-cool-heat cycle was run on each sample. The first heat cycle was used to erase any thermal history, and the second heat cycle was used to measure the T_g and T_m values. The samples were heated to 250 °C and cooled to −90 °C at a rate of 10 °C/min. The average was taken for each set of three samples per color.

2.4 Thermogravimetric Analysis. Thermogravimetric analysis (TGA) measured the point of onset degradation and the change in mass of the specimen over a temperature sweep. The temperature was increased from room temperature to 600 °C at 10 °C/min under nitrogen atmosphere. The TGA tests were performed using a high-temperature platinum pan.

2.5 Rheology. Rheological characterization was investigated using parallel plates with environmental testing chamber. Frequency sweeps were conducted at 500–0.1 rad/s with constant strain of 0.5% at 200 °C. Temperature sweeps were performed from 200 °C to 100 °C at 3 °C/min with a constant frequency of 10 rad/s and strain of 0.5%. Printed samples had a 2 mm thickness and 25 mm diameter and the rheological testing gap was 1.5 mm.

2.6 Crystallinity From X-ray Diffraction. X-ray diffraction (XRD) investigated crystallinity. Circular samples were cut from printed squares with scissors to serve as XRD samples. Samples in each color and blue samples printed at nozzle temperatures 185 °C, 200 °C, and 210 °C were tested. The XRD used Co Kα with run conditions of 40 kv and 45 mA.

2.7 PETG Prints. Printed PETG samples were also tested in the water bath following using the same procedure outlined for the PLA samples. The water temperature was 85 °C. Three samples from each print bed location (left, right, and middle) were tested.

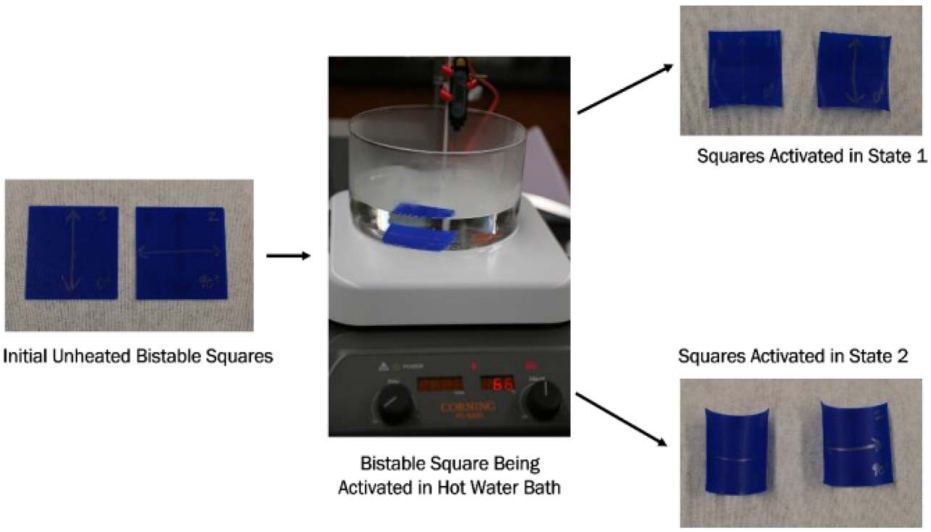

Fig. 2 Process of sample activation to state 1 or state 2

Table 1 Percentage bistability based on filament print color

Color	Number of bistable samples (out of three samples)	Percentage bistable
Clear pro	3	100%
Blue	2	67%[a]
Green	2	67%[b]
Purple	1	33%
Black	0	0%
Lime green	0	0%
Yellow	0	0%
Red	0	0%

[a]Blue PLA was expected to be 100%.
[b]Scraggly corner in one sample could explain lack of bistability in one sample.

3 Results and Discussion

3.1 Water Bath Heating Test for Bistability Results and Discussion. Because the bistability displayed by the samples existed as a range, bistability for a color was based on the ratio of bistable samples to total samples (i.e., if two samples were bistable out of three total samples = 2/3 = 67%). The results are shown in Table 1. As shown in Table 1, four colors exhibited some amount of bistability, and four colors did not exhibit bistability. The clear pro filament had the most consistent bistable samples at 100%. The blue and green filament exhibited 67% bistability. Then, the purple filament exhibited 33% bistability. The black, lime green, red, and yellow filaments exhibited no bistability at the given print setting. The samples varied in ease of switching states and speed to return to original state, if monostable. Yellow samples returned to the first state quickly, while monostable samples of the black, red, and lime green filament returned more slowly.

Bistability is partially dependent on filament color. The colorant and other additives affect the polymer chain behavior during the printing and cooling process. The filament colors that exhibited bistability did not consistently exhibit bistability across all samples. The variability within each potentially bistable color could be caused by slight differences in over- or under-extrusion. Seven of eight colors had a filament diameter tolerance of ±0.05 mm [22,25], of which three had some bistable behavior. One color, clear pro, had a tolerance of ±0.02 mm [21] and demonstrated the most consistent bistability. Given that a smaller tolerance allows for more consistent extrusion with less over- and under-extrusion during the print process [27], pre-strain may have been stored more evenly and consistently within the print, allowing for more accurate prints. More research is needed to conclusively determine the effect of filament diameter tolerance on pre-strain storage.

3.2 Differential Scanning Calorimetry Results and Discussion. The average values of T_g and T_m are shown in Table 2, with colored filament ordered along decreasing T_g.

Table 2 T_g and T_m of filament colors in decreasing T_g order

MatterHackers PLA filament color	Average temperature in °C		Percentage bistability (out of three samples)
	T_g	T_m	
Red	60.72	175.44	0%
Blue	59.48	169.77	67%
Yellow	58.13	172.87	0%
Black	57.86	175.29	0%
Lime green	57.54	174.44	0%
Green	56.96	167.02	67%
Purple	56.93	169.46	33%
Clear pro	55.69	150.75	100%

A clear trend for T_g is not evident. All samples that display some bistability are in the lower half of the T_m values, but a correlation between percentage of bistability and increasing or decreasing T_m is not observed. Further study of a wide variety of colors across different filament companies could determine whether a trend exists for T_g and whether the trend for T_m continues to hold. Having a lower T_m could be advantageous during the pre-strain storage process. The heating and cooling behavior of the filament during the printing process likely has a strong effect on the pre-strain storage process, indicating that nozzle temperature and print bed temperatures may be important factors.

3.3 Thermogravimetric Analysis Results and Discussion. Figure 3 shows the behavior of all eight colors when heated to degradation. There was no visible trend between TGA results, filament color, and bistable behavior. Two distinct behaviors can be seen. Blue and clear pro filaments exhibit 100% mass loss. The other colors exhibit about 90% mass loss, where the residual material could be the colorant.

The type and amount of colorant used to dye the filament likely affect its T_g and T_m. The colorant likely affects the hydrogen bonds and van der Waals forces between the polymer chains, which could change the T_g and T_m and affect any crystallization or entanglement process in the material and thereby the resulting SME behavior. The black filament likely uses carbon black, and the blue filament is likely a variant of anthraquinone dye. The other colors may also be a variant of anthraquinone dye.

The colorant effect on material properties makes colorant choice instrumental in designing metamaterials with consistent bistable development at given print parameters. Knowing the colorant and how it affects PLA will be paramount for future design; however, filament producers are unlikely to share colorant type and amount, making the study challenging. Filament additives could be designed to enhance the pre-strain development.

3.4 Rheology Results and Discussion. Oscillatory frequency sweeps were conducted at the print temperature of 200 °C to characterize the viscoelasticity of the material during extrusion. The results are shown in Fig. 4. For all filament colors, $G'' > G'$ over the range of frequencies tested and indicates the material is behavior is dominated by the viscous response. The filaments have observed terminal behavior with red exhibiting some deviation of expected Newtonian behavior.

To further understand the thermal effects on viscoelasticity, oscillatory temperature sweeps were completed. Figure 5 summarizes the temperature sweep data. Beginning at 200 °C, $G'' > G'$ and the material behaves as viscous liquid. As the material is cooled, modulus crossover where G' dominates is observed. The crossover temperatures (T_{cross}) are color dependent as shown in Table 3. For clear pro, green, and purple, the data are smooth throughout the cooling temperature ramps. Other colors experienced rapid changes past the crossover temperature and almost a solidification. For example, the blue data exhibited the highest T_{cross} and had very sharp transition. The normal axial force readings increased dramatically during the modulus crossover to cause the data to be errant. Similar behaviors are observed for black, lime green, red, and yellow.

The rheology did not reveal a defining feature for bistable colors. Clear pro, with 100% bistability, showed a smooth profile, while blue, with 67% bistability, showed a sudden jump. Blue had the highest T_{cross} and green had the lowest T_{cross} of bistable samples. Both blue and green showed some bistability, indicating that T_{cross} does not distinguish between bistable and monostable. The sharp drop in viscosity may allow a material to hold more pre-strain as it cools.

3.5 Crystallinity Results and Discussion. As shown in Fig. 6, blue and clear pro samples were fully amorphous; all other samples

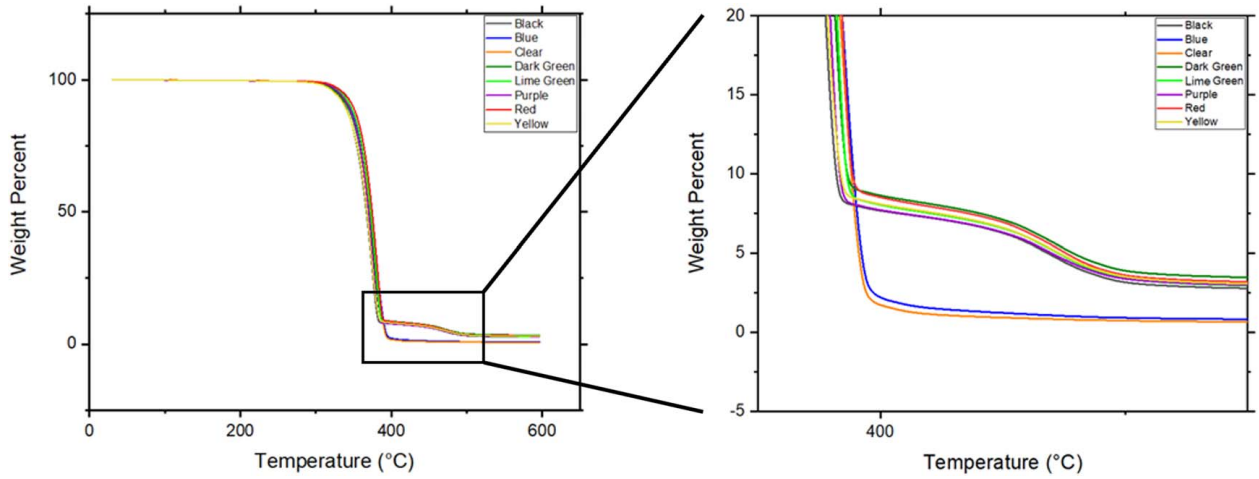

Fig. 3 TGA data from PLA filament

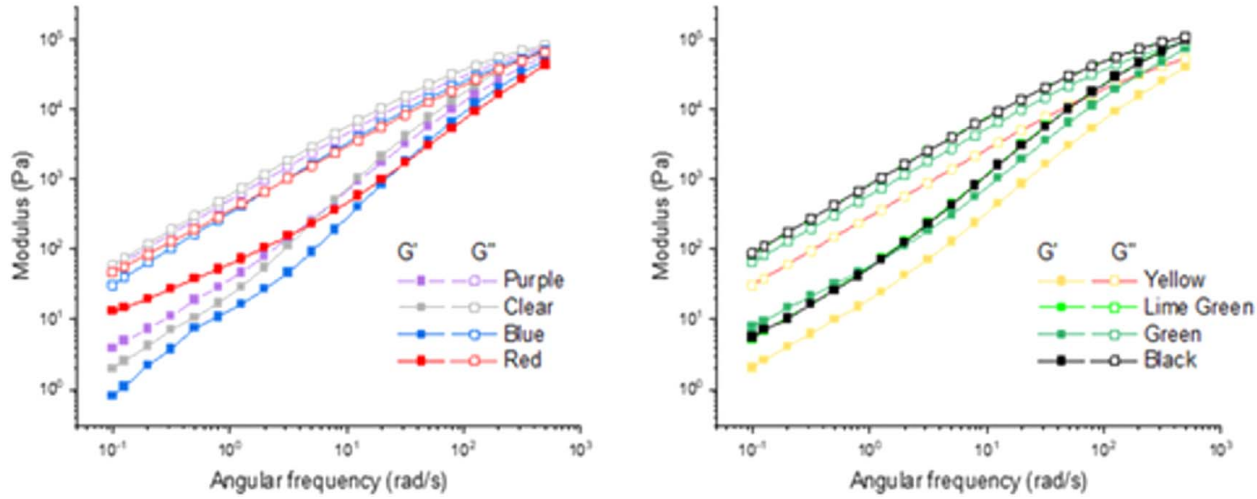

Fig. 4 Frequency sweeps at 200 °C of PLA filaments

had some crystallinity in the form of calcite ($CaCO_3$). The sample labeled teal is another green sample.

Figure 7 shows the blue filament samples at three different nozzle temperatures. The 185 °C had a significant peak not seen in the other samples. Preliminary work from left, right, and middle prints showed strong evidence for blue samples being bistable between 185 °C and 200 °C. (Clear Pro had evidence of bistability between 195 °C and 215 °C, excluding 205 °C. Black showed evidence of bistability at 185 °C.) False negatives occurred from printing on the left, right, and middle of the print bed; however, there is evidence that nozzle temperature affects bistability. As temperature increased, PLA may have lost some of its crystallinity, appearing amorphous.

Wittbrodt and Pearce found a difference in percent crystallinity for both filament color and nozzle temperature. The current work validates that both differences occur; however, the XRD results have not been tied to the crystalline portion of the semi-crystalline PLA. More research is needed to determine the percentage of crystallinity in PLA.

3.6 PETG Results and Discussion. None of the PETG samples exhibited bistability at the given print parameters; all exhibited the SME and all samples curled up toward the bilayer90 in state 2, away from bilayer0. Soleyman et al. stated that the highest pre-strain is on the bottom layer of the print due to their samples bending downward to the side printed closest to the print bed [16], which seems unlikely. First, Soleyman et al. appeared to use an alternating 0 deg/90 deg for a thickness of 1 mm at 0.2 mm layer height (three layers of 0 deg and two layers of 90 deg) [16]. Soleyman et al. had an extra layer for each print, which could predispose the print to bend toward the direction with more layers (the bottom layer) giving the impression of higher pre-strain on the bottom. The monostable PETG samples had an equal number of layers (five layers of 0 deg and then five layers of 90 deg), resulting in more equal comparison. Finally, Soleyman et al. used a bed temperature of 60 °C [16] whereas this paper used 85 °C as the print bed temperature. The higher bed temperature may have relaxed more of the pre-strain in the bottom layers and resulted in a behavior closer to what was seen in Bodaghi et al. with PLA [12], with the most pre-strain in the top layer. With parameter tuning, PETG could be a viable option for printing SMS.

3.7 General Discussion. All tested samples demonstrated SME; only some displayed bistability. Extensive material testing could not find a definitive trend between material and bistability. The SME relies on both material and process [9]. Any material that exhibits SME and can be FDM printed is expected to have a set of print parameters that would create bistability; likewise, with proper tuning, bistability can likely be created for most

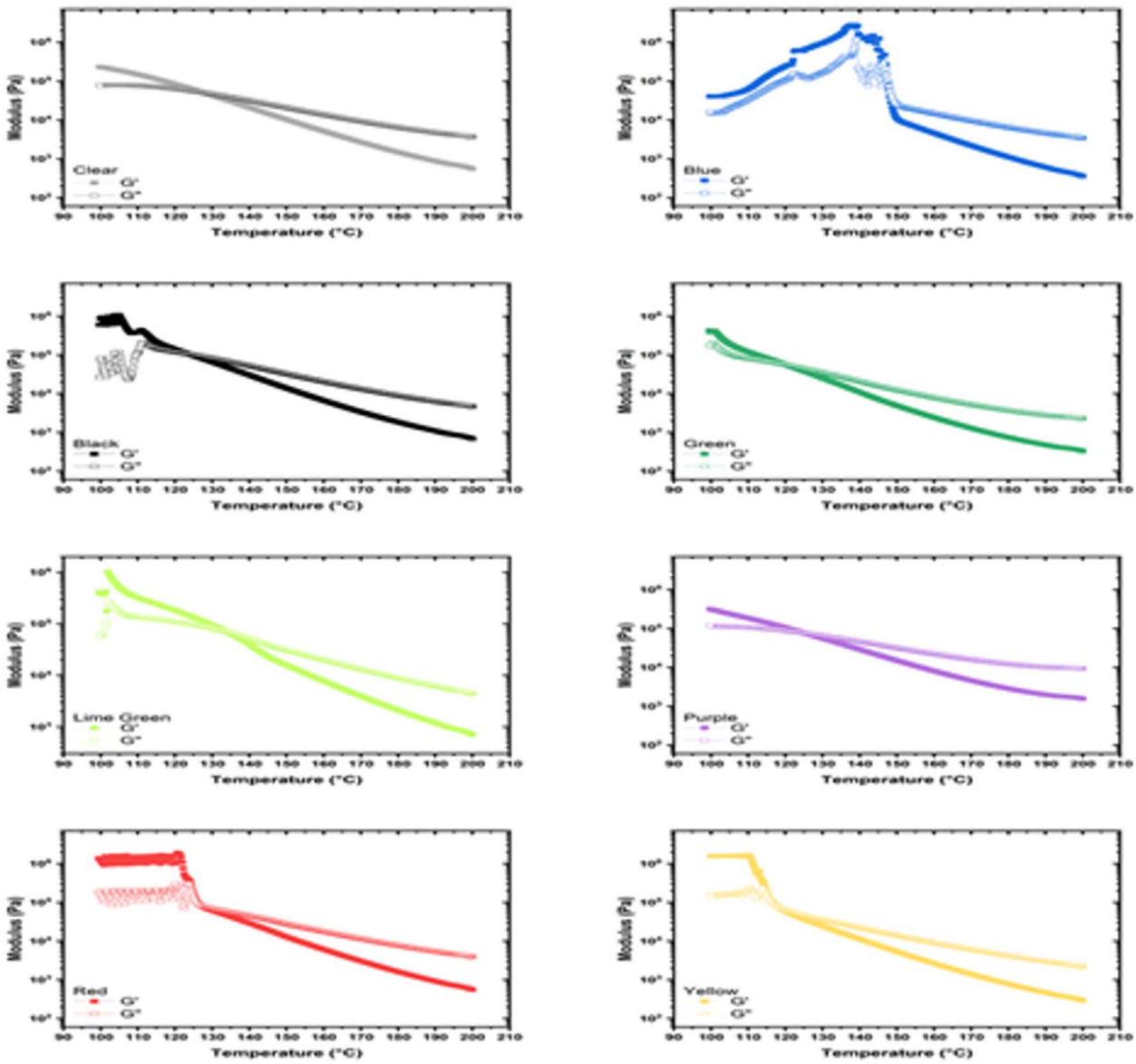

Fig. 5 Viscoelastic oscillation temperature sweeps for the eight PLA filaments

Table 3 G'/G'' crossover temperatures (T_{cross}) for filament colors

PLA filament color	G'/G'' crossover temperature (°C) T_{cross}
Blue	147.28
Lime green	134.19
Clear	127.5
Red	127.26
Purple	125.07
Black	123.82
Green	120.14
Yellow	118.16

SMP color and additive variations. Any colorant or additive added to the base material affects the shape-fixing and/or the shape-switching element, affecting the pre-strain stored. To draw conclusions about chemical interactions, specifics on base material and colorant are needed, which will be challenging given the proprietary nature of both. Given that different processing settings are needed for different materials, printers with two nozzles or more allow for multiple print parameters to be used to create bistable behavior for multi-material SMS, as demonstrated in Riley et al. [6].

3.8 Mathematical Explanation. A possible mathematical explanation is provided for bistability. Pre-strain storage and release will be described during the printing and the activation process. Then the theory will be applied to a square with bilayers during activation. Finally, an explanation for bistability is presented.

During the printing process, one bead of material is laid down at a time. That bead is stretched and then cools, storing pre-strain. A series of beads printed at the same distance from the print bed are a printed layer. Assume that a bead printed on the same layer in the same direction with the same print parameters has the same pre-strain as all others on the same layer. Finally, assume that the pre-strain stored is equivalent to some potential energy related to stretched amorphous polymer chains. The process can be viewed in terms of bead, layer, bilayer, or as an entire structure. The interaction between the printed beads will not be considered below.

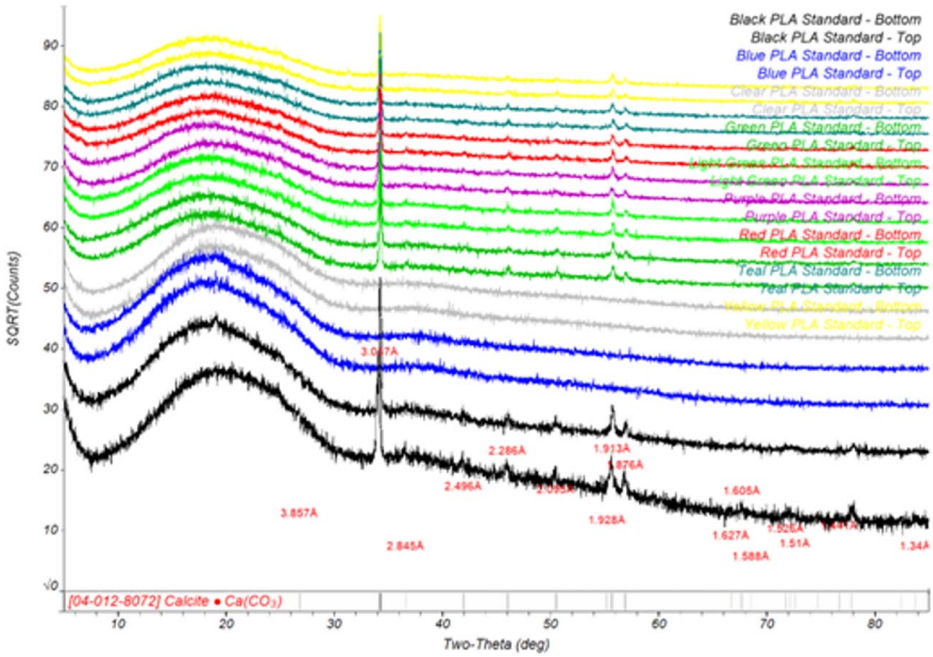

Fig. 6 XRD results of top and bottom layers of printed samples

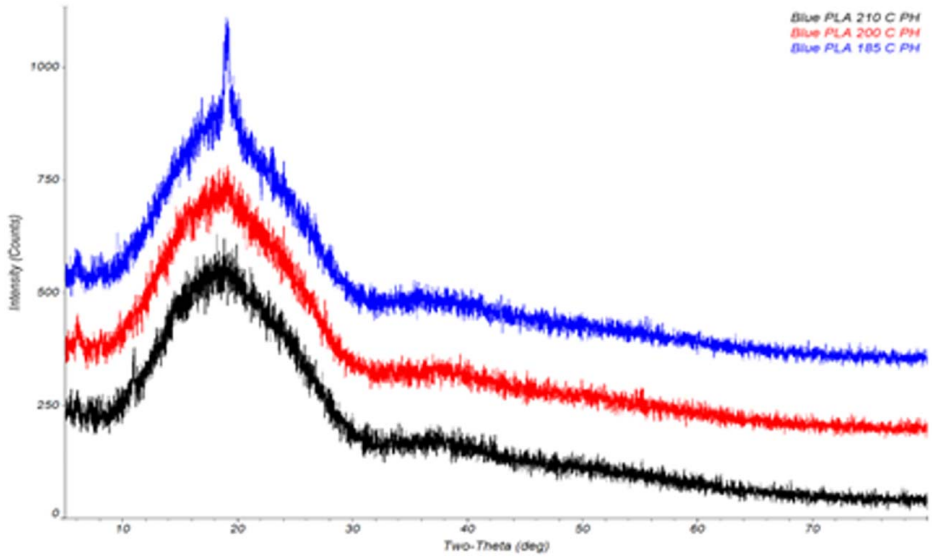

Fig. 7 XRD of blue PLA printed samples at three different temperatures

The energy is provided during the printing process, when the polymer is fixed in an energetically unfavorable state. The energy provided during the initial printing is e_{initial}. Some energy is lost before the print cools below T_g for the first time and additional energy is lost when a new layer reheats the cooled layer below it or from heat applied by the print bed. The energy can be broken into multiple terms due to the repeated heating and cooling process; however, the energy lost during the entire process will be considered in one term: e_{lost}. Once the print is complete and cooled below T_g, there will be some energy stored, e_{stored}. When the print is heated above T_g during activation, the polymer will shrink, releasing some energy, e_{released}. When the print is cooled below T_g again, there is some remaining or left energy, e_{left}. The print can be repeatedly heated above and cooled below T_g, where e_{left} and e_{released} can be in parts or as a global value. Equation (1) refers to the initial energy storage process, Eq. (2) refers to the energy release during the shape recovery process, and Eq. (3) refers to the total process.

$$e_{\text{initial}} = e_{\text{lost}} + e_{\text{stored}} \tag{1}$$

$$e_{\text{released}} = e_{\text{stored}} - e_{\text{left}} \tag{2}$$

$$e_{\text{initial}} = e_{\text{lost}} + e_{\text{released}} + e_{\text{left}} \tag{3}$$

Assume there is a maximum possible e_{initial}, driven by printer parameters and given material, and a minimum possible e_{left} that must remain in a given layer. Therefore, there is a range of possible e_{stored} and there is a maximum e_{released} limited by print parameters and material, as established in Eq. (4)

$$e_{\text{released}} \leq e_{\text{initial,max}} - e_{\text{left,min}} \tag{4}$$

Now the reheating process during the printing process will be considered more closely. Each layer of a print has its own e_{stored}.

The e_{stored} for each layer will be measured starting at 1 and ending at n, with n being the maximum number of layers in the print. There are four elements that comprise e_{stored}: e_{intial}, $e_{lost,initial}$ (which refers to the pre-strain lost during the initial extrusion), $e_{lost,printbed}$ (which refers to the pre-strain lost due to the print bed), and $e_{lost,reheat}$ (which refers to the pre-strain lost due the reheating from the nozzle). $e_{lost,printbed}$ and $e_{lost,reheat}$ are both functions of distance. The further a printed layer, layer i, is from the print bed, the less heat the layer will receive and the smaller $e_{lost,printbed}$ will be. Likewise, the further layer i is from the most recently extruded layer, the less heat the layer will receive from the extrusion and the smaller $e_{lost,reheat}$ will be. For simplicity, $e_{initial}$ and $e_{lost,initial}$ will be considered constant across all layers, even though there may be some variation.

There exists an equation that describes the how the print bed affects the energy stored in a layer, given the distance from the layer to the print bed ($d_{printbed}$), the material properties ($p_{material}$), the print bed temperature ($T_{printbed}$), the temperature of the layer i ($T_{layer,i}$), and the effect of print parameters (p_{print}), shown in Eq. (5). There exists a distance, ($d_{printbed,final}$), where the heating effect from the heat bed is negligible. The print bed is assumed to heat consistently across time and distance, though this is not often the case. If the print bed is off, $e_{lost,printbed}$ is 0.

$$e_{lost,printbed} = f(d_{printbed}, T_{printbed}, T_{layer}, p_{material}, p_{print}) \quad (5)$$

There is an equation that describes how a newly extruded layer, z, affects the energy stored in a layer i, given the distance from the new layer ($d_{printedlayer}$), the temperature of the new printed layer ($T_{printed\ layer}$), the temperature of the layer i ($T_{layer,i}$), the material properties ($p_{material}$), and the effect of print parameters (p_{print}), shown in Eq. (6). There is a distance at which the effect of the newly printed layer is insignificant, denoted by $d_{printedlayer,final}$. Layers repeatedly affected by the reheating effect will lose more pre-strain than those that have less exposure to reheating (layers in the upper portion of a print).

$$e_{lost,reheat,i,z} = f(d_{printedlayer}, T_{printedlayer}, T_{layer,i}, p_{material}, p_{print}) \quad (6)$$

Another way to consider the printing process is to look at the temperature of the layer above (T_{i+1}) and the layer below (T_{i-1}) as well as the material properties and print parameters, shown in Eq. (7). This method will not be given much consideration in this work.

$$e_{lost,layerprinting} = f(T_{i+1}, T_{i-1}, p_{material}, p_{print}) \quad (7)$$

The time it takes the printer to complete a layer will affect the reheating process. This is considered in the print parameters, which includes the print speed and can be extended to include the design of each layer. It may also be considered as a separate element. Given that a bistable square has the same shape and the same print speed for each layer, the time needed to complete each layer is considered the same; therefore, time needed to print a layer is not included directly.

Consider a print of exactly three layers. Layer 1 is directly on the print bed, layer 3 is the top layer, and layer 2 is between layers 1 and 3. Therefore layer 1 will lose the most pre-strain energy due to print bed and the reheating process and layer 3 will lose the least, as shown in Eqs. (8) and (9), respectively:

$$e_{lost,printbed,1} > e_{lost,printbed,2} > e_{lost,printbed,3} \quad (8)$$

or

$$e_{lost,reheat,total,1} > e_{lost,reheat,total,2} > e_{lost,reheat,total,3} \quad (9)$$

Equations (10)–(12) describe the total e_{stored} due to layer position. Equation (12) does not contain a reheat element because no energy is lost to reheating in the top layer.

$$e_{stored,1} = e_{initial} - e_{lost,initial} - e_{lost,print\ bed,1} - e_{lost,reheat,1,2} - e_{lost,reheat,1,3} \quad (10)$$

$$e_{stored,2} = e_{initial} - e_{lost,initial} - e_{lost,print\ bed,2} - e_{lost,reheat,2,3} \quad (11)$$

$$e_{stored,3} = e_{initial} - e_{lost,initial} - e_{lost,printbed,3} \quad (12)$$

Layer 1 will lose the most pre-strain, resulting in the least energy stored and layer 3 will have most energy stored, having lost the least pre-strain, as shown in Eq. (13).

$$e_{stored,1} < e_{stored,2} < e_{stored,3} \quad (13)$$

Or more generally in Eq. (14)

$$e_{stored,1} < e_{stored,i} < e_{stored,n} \quad (14)$$

This conclusion aligns with Bodaghi et al., Nozoori et al., and Tezerjani et al. [12,14,15], where the pre-strain is the greatest at the top layer and least at the bottom.

Now consider a switchable bistable square with ten layers, which are labeled 1–10, starting at the print with 1 and ending at the top layer with 10. Layers 1–5 are printed in the 0 deg direction. Layers 6–10 are printed in the 90 deg direction. Assume that layers printed in the same direction form a bilayer and the energy stored can be considered globally for the bilayer. The square can be described with $e_{stored,bilayer0}$ and $e_{stored,bilayer90}$, with bilayer0 containing layers 1–5 and bilayer90 containing layers 6–10. Further assume that a bistable square above T_g requires a given energy (e_{snap}) to snap between states and that the T_{act} has negligible effect on the required e_{snap}, as long as $T_m > T_{act} > T_g$. Note that the energy required to snap a bistable square below T_g is infinite because the sample will break before it is snapped between states. Also note that $e_{stored,bilayer90}$ is generally greater than $e_{stored,bilayer0}$, assuming bilayer90 is the top layer.

When a bistable square is activated, the sample will self-snap without external force. The as-printed shape is the temporary shape and the snapping is a result of the sample shrinking and switching to one of its stable states. There are three common options: (1) the sample will fully self-snap to one state; (2) the sample will self-snap toward a state and then self-snap fully to the opposite state; and (3) the sample will self-snap to an in-between state and will stay there until an external force provides energy to complete the snap in one direction. Because the sample started flat and in its temporary shape, a lower $e_{snap,initial}$ is overcome.

Equation (15) describes the instantaneous energy release rate, r_i, where t_i is the time at a given moment and $e_{released,ti}$ is the energy released at t_i. Equation (16) looks at the total energy release rate from the initial start time until that moment, $r_{released}$, and models the current state of snapping, where the total energy released is $e_{released}$, the start time is t_0, the energy stored at t_0 is $e_{stored,t0}$, and the energy stored at t_i is $e_{stored,ti}$. Equation (17) looks the final energy released, $r_{released,final}$, once the snapping behavior has stabilized and serves to look at the global behavior, where the final time is t_f, the energy released is $e_{released,final}$, and the energy stored at t_f is $e_{stored,tf}$.

$$r_i = \frac{e_{released,t_i}}{t_i} \quad (15)$$

$$r_{released} = \frac{e_{released}}{t_i - t_0} = \frac{e_{stored,t_0} - e_{stored,t_i}}{t_i - t_0} \quad (16)$$

$$r_{released,final} = \frac{e_{released,final}}{t_f - t_0} = \frac{e_{stored,t_0} - e_{stored,t_f}}{t_f - t_0} \quad (17)$$

For case 1, the difference in the material shrinkage is sufficiently large that one bilayer dominates, causing a full self-snap. For case 2, the shrinkage varies, with one bilayer having greater energy released for a time until the opposite bilayer releases enough energy to fully transition. For case 3, the energy difference between the layers is not initially sufficient to fully snap. The difference in bilayer energy over the period in which the snapping occurs (whether instantaneous or long term) determines which direction

the sample snaps. The initial shrinkage is sufficient to overcome $e_{\text{snap,initial}}$ or to establish a tenuous balance between states, indicating the pre-strain release is the highest in the initial activation. This is corroborated by Riley et al., who demonstrated that a blue PLA filament printed at 0.01 mm layer height exhibited pre-strain shrinkage of about 0.05 mm/mm within the first 30 s and achieved a total pre-strain shrinkage of 0.08 mm/mm by 300 s [6]. Case 1 was the most common, with case 2 and case 3 being less common. This implies that there is a difference in pre-strain in even identical appearing prints. When viewed globally, Eqs. (18)–(19) apply to case 1 and case 2.

$$\frac{e_{\text{released},f,\text{bilayer0}}}{t_f - t_0} < \frac{e_{\text{released},f,\text{bilayer90}}}{t_f - t_0} \tag{18}$$

or

$$\frac{e_{\text{released},f,\text{bilayer0}}}{t_f - t_0} > \frac{e_{\text{released},f,\text{bilayer90}}}{t_f - t_0} \tag{19}$$

The sample will most often snap in the bilayer90 direction in case 1, with bilayer90 being the top layer in this case, correlating with the idea that more pre-strain is stored at the top layer of printing [12,14,15]; however, some prints will initially snap to bilayer0 or will exhibit case 2 or 3, indicating that having higher pre-strain storage at the top layers is more likely, though the gradient between the top and bottom layer may not always be large, even for prints with the same parameters.

When viewed globally, case 3 can be described by Eq. (20), indicating that the energy released was approximately equal.

$$\frac{e_{\text{released},f,\text{bilayer0}}}{t_f - t_0} \approx \frac{e_{\text{released},f,\text{bilayer90}}}{t_f - t_0} \tag{20}$$

To snap a sample in case 3, perhaps to bilayer90, a pair of tweezers is used, which is referred to in Eq. (21) as e_{external}. The time for the snap is considered instantaneous, even though the actual snapping takes a few seconds and a couple tries.

$$e_{\text{released,bilayer0}} < (e_{\text{released,bilayer90}} + e_{\text{external}}) \tag{21}$$

Now assume that the sample is above T_g and snapped to bilayer90. Tweezers will apply an external force to snap the sample to bilayer0. Consider the moment of the snap, denoted $t_{\text{snap},m}$. The snap is not instantaneous but can be assumed to be given that the energy applied by the tweezers is significantly greater than any energy stored in the sample, as shown in Eq. (22).

$$e_{\text{external}} > e_{\text{released}}(t_{\text{snap},m}) \tag{22}$$

If the sample is bistable, it will stay at bilayer0 until it is snapped again or it is lowered below T_g, where the material becomes glassy. More specifically, the energy difference in the bilayers is less than the energy needed to overcome e_{snap}, as shown in Eqs. (23) and (24):

$$|e_{\text{bilayer0}} - e_{\text{bilayer90}}| < e_{\text{snap}} \tag{23}$$

or

$$\left|\frac{e_{\text{bilayer0}}}{t_{\text{return}}} - \frac{e_{\text{bilayer90}}}{t_{\text{return}}}\right| < \frac{e_{\text{snap}}}{t_{\text{return}}} \tag{24}$$

where t_{return} is defined as the time from the completion of the last snap until the next snap is initiated by an external force or a self-snap is completed.

If the sample is monostable, the energy difference between the bilayers is greater than e_{snap}, as shown in Eqs. (25) and (26).

$$|e_{\text{bilayer0}} - e_{\text{bilayer90}}| > e_{\text{snap}} \tag{25}$$

or

$$\left|\frac{e_{\text{bilayer0}}}{t_{\text{return}}} - \frac{e_{\text{bilayer90}}}{t_{\text{return}}}\right| > \frac{e_{\text{snap}}}{t_{\text{return}}} \tag{26}$$

The faster the return, the faster the release of pre-strain energy occurs and the greater the difference in the pre-strain energy is. The pre-strain in one bilayer is released a little faster on one side than the other, causing shrinkage, until the energy threshold of e_{snap} is reached and the return self-snap occurs.

Finally, if a sample is left at T_g for an extended period of time, $e_{\text{left,min}}$ will be reached. When the external force is applied, the sample will return to the state that has become the fixed permanent state due to pre-strain release.

Pre-strain storage is affected by multiple parameters, implying that it is possible to either increase e_{snap} or decrease the bilayer energy difference to allow for bistability in a wide variety of materials, colors, and print parameters, inviting further study. The pre-strain for each bead was assumed to be equal to the one next to it. This is not true, given the difference in filament tolerance and having two beads on the edge always exposed to outside air. Determining the effect of filament tolerance on the consistency of stored pre-strain and varied print bed temperature on pre-strain gradient will be important.

Measuring the pre-strain stored during the printing will be challenging. Pre-strain shrinkage tests like those used in Riley et al. can show the e_{released}, related to e_{stored} by Eq. (2), likely sufficient for understanding bistable behavior on a practical level. The broader equations provide a framework tying the molecular, single layer, bilayer, and macro behavior with the variance caused by material, color, and print parameters and could be extended to a computer model of the printing process.

The inherent variability in the pre-strain storage process during must be considered during sample creation. Using filament with finer tolerance may result in more consistent bistability and could potentially limit the effect of color. Extrusion behavior at the nozzle, affected by material and extruder design, may have some effect on pre-strain storage. Controlling variance will create more consistent SMS allowing transition to application.

4 Conclusion

A bistable square has a pre-strain difference in its bilayers that is unable to overcome e_{snap}, which is determined by the pre-strain stored in each layer, which depends on many inter-reliant factors, one of which is color. A combination of print parameters and material choices likely exists that would allow bistable behavior for most SME 3D printable materials. A series of mathematical equations can describe the pre-strain storage and release process as well as whether a sample is bistable or monostable. Careful consideration of material and process is required when creating 4D printed pre-strain driven structures, and more research is needed to understand the pre-strain storage process and causes of variance during printing.

Acknowledgment

The tests described and the resulting data presented herein, unless otherwise noted, are based on work conducted by the U.S. Army ERDC supported under 511633/H06F0F "Autonomous Digital Design." Permission was granted by the Director, Geotechnical and Structures Laboratory to publish this information. The findings of this report are not to be construed as an official Department of the Army position unless so designated by other authorized documents.

 Research was inspired by the work completed in Riley et al. [6].

Conflict of Interest

There are no conflicts of interest. This article does not include research in which human participants were involved. Informed consent was not applicable. This article does not include any research in which animal participants were involved.

Data Availability Statement

The datasets generated and supporting the findings of this article are obtainable from the corresponding author upon reasonable request.

References

[1] Zhang, Z., Demir, K. G., and Gu, G. X., 2019, "Developments in 4D-Printing: A Review on Current Smart Materials, Technologies, and Applications," Int. J. Smart Nano Mater., **10**(3), pp. 205–224.

[2] International Organization for Standardization, 2014, "*Additive Manufacturing : General Principles Part 3: Main Characteristics and Corresponding Test Methods*," ISO.

[3] Mitchell, A., Lafont, U., Hołyńska, M., and Semprimoschnig, C., 2018, "Additive Manufacturing—A Review of 4D Printing and Future Applications," Addit. Manuf., **24**, pp. 606–626.

[4] Matos, B. D. M., Rocha, V., da Silva, E. J., Moro, F. H., Bottene, A. C., Ribeiro, C. A., dos Dias, D. S., et al., 2019, "Evaluation of Commercially Available Polylactic Acid (PLA) Filaments for 3D Printing Applications," J. Therm. Anal. Calorim., **137**(2), pp. 555–562.

[5] Spina, R., 2019, "Performance Analysis of Colored PLA Products With a Fused Filament Fabrication Process," Polymers, **11**(12), p. 1984.

[6] Riley, K. S., Ang, K. J., Martin, K. A., Chan, W. K., Faber, J. A., and Arrieta, A. F., 2020, "Encoding Multiple Permanent Shapes in 3D Printed Structures," Mater. Des., **194**, p. 108888.

[7] van Manen, T., Janbaz, S., and Zadpoor, A. A., 2017, "Programming 2D/3D Shape-Shifting With Hobbyist 3D Printers," Mater. Horiz., **4**(6), pp. 1064–1069.

[8] Momeni, F., Hassani, N. S. M. M., Liu, X., and Ni, J., 2017, "A Review of 4D Printing," Mater. Des., **122**, pp. 42–79.

[9] Lendlein, A., and Kelch, S., 2002, "Shape-Memory Polymers," Angew. Chem. Int. Ed., **41**(12), pp. 2034–2057.

[10] Sobota, M., Jurczyk, S., Kwiecień, M., Smola-Dmochowska, A., Musioł, M., Domański, M., Janeczek, H., Kawalec, M., and Kurcok, P., 2017, "Crystallinity as a Tunable Switch of Poly(L-Lactide) Shape Memory Effects," J. Mech. Behav. Biomed. Mater., **66**, pp. 144–151.

[11] Yahia, L., 2015, *Shape Memory Polymers for Biomedical Applications*, Elsevier, New York.

[12] Bodaghi, M., Noroozi, R., Zolfagharian, A., Fotouhi, M., and Norouzi, S., 2019, "4D Printing Self-Morphing Structures," Materials, **12**(8), p. 1353.

[13] Mehrpouya, M., Vahabi, H., Janbaz, S., Darafsheh, A., Mazur, T. R., and Ramakrishna, S., 2021, "4D Printing of Shape Memory Polylactic Acid (PLA)," Polymer, **230**, p. 124080.

[14] Noroozi, R., Bodaghi, M., Jafari, H., Zolfagharian, A., and Fotouhi, M., 2020, "Shape-Adaptive Metastructures With Variable Bandgap Regions by 4D Printing," Polymers, **12**(3), p. 519.

[15] Tezerjani, S. M. D., Yazdi, M. S., and Hosseinzadeh, M. H., 2022, "The Effect of 3D Printing Parameters on the Shape Memory Properties of 4D Printed Polylactic Acid Circular Disks: An Experimental Investigation and Parameters Optimization," Mater. Today Commun., **33**, p. 104262.

[16] Soleyman, E., Rahmatabadi, D., Baniassadi, M., and Baghani, M., 2022, "Effect of Printing Parameters on the Shape Transformation of 3D Printed PETG," The 30th Annual International Conference of Iranian Society of Mechanical Engineers, Tehran, Iran, May 10–12.

[17] Aberoumand, M., Soltanmohammadi, K., Soleyman, E., Rahmatabadi, D., Ghasemi, I., Baniassadi, M., Abrinia, K., and Baghani, M., 2022, "A Comprehensive Experimental Investigation on 4D Printing of PET-G Under Bending," J. Mater. Res. Technol., **18**, pp. 2552–2569.

[18] Charvat, R. A., 2003, *Coloring of Plastics*, John Wiley & Sons, Hoboken, NJ.

[19] Wittbrodt, B., and Pearce, J. M., 2015, "Effects of PLA Color," Addit. Manuf., **8**, pp. 110–116.

[20] Cao, Y., Derakhshani, M., Fang, Y., Huang, G., and Cao, C., 2021, "Bistable Structures for Advanced Functional Systems," Adv. Funct. Mater., **31**(45), p. 2106231.

[21] MatterHackers, "Translucent Clear PRO Series PLA Filament-1.75 mm (1 kg) | MatterHackers," MatterHackers. https://www.matterhackers.com/store/l/pro-series-pla/sk/MESZ27MX, Accessed March 31, 2023.

[22] MatterHackers, "Blue MH Build Series PLA Filament—1.75 mm (1 kg)_ MatterHackers," MatterHackers. https://www.matterhackers.com/store/3d-printer-filament/175mm-pla-filament-blue-1-kg, Accessed March 31, 2023.

[23] Prusa 3D Printers, "Original Prusa I3 MK3S+ Kit_Original Prusa 3D Printers Directly From Josef Prusa," Original Prusa 3D printers directly directly from Josef Prusa. https://www.prusa3d.com/product/original-prusa-i3-mk3s-kit-3/

[24] MatterHackers, "Technical Data Sheet—Build Series PETG."

[25] MatterHackers, "3D Printing Filament: Technical Data Sheet—Build Series PLA."

[26] Quintana, J. L. C., Slattery, L., Pinkham, J., Keaton, J., Lopez-Anido, R. A., and Sharp, K., 2022, "Effects of Fiber Orientation on the Coefficient of Thermal Expansion of Fiber-Filled Polymer Systems in Large Format Polymer Extrusion-Based Additive Manufacturing," Materials, **15**(8), p. 2764.

[27] Cardona, C., Curdes, A. H., and Isaacs, A. J., 2016, "Effects of Filament Diameter Tolerances in Fused Filament Fabrication," IU J. Undergrad. Res., **2**(1), pp. 44–47.